Solar Foundation Design in Cold Climates

Newson, T. & Hammad, M.
Department of Civil & Environmental Engineering, University of Western Ontario, London, Ontario, Canada
Davies, M.C.R.
School of Mathematics, Computer Sciences & Engineering, City University of London, London, United Kingdom and University of Sussex, United Kingdom
Yazdani, A., Kuepfer, G. & Mendosa, J.
PRI Engineering Corp, Lindsay, Ontario, Canada.

GeoCalgary 2022 October 2-5
Reflection on Resources

ABSTRACT
Foundations for solar power plants present unique design challenges, requiring large numbers of small, closely spaced piles. Since the piles are relatively short, near surface climatic effects, such as seasonal ground freezing and wind loading, can lead to heaving and deformation of the piles that can lead to damage to the above-grade racking system which support the photovoltaic (PV) modules. This paper describes a study based on field data from axial and lateral load tests, which were conducted for an existing solar project, to predict the overall movement and other design parameters using both a code-based approach and the semi-empirical analytical method, proposed by Ladanyi and Foriero (1998), that uses the well-established modified Berggren equation, (Aldrich and Paynter, 1953) to calculate the dept of freezing. This has allowed an assessment of current design methods and more insight into the routine calculation of the rate of frost penetration and heave, resulting in pile uplift forces. The study has revealed aspects that require further study to facilitate practical, economic design, and recommendations for future research to address these aspects are made.

RÉSUMÉ
Les fondations des centrales solaires présentent des défis de conception uniques, nécessitant un grand nombre de petits pieux rapprochés. Étant donné que les pieux sont relativement courts, les effets climatiques proches de la surface, tels que le gel saisonnier du sol et la charge du vent, peuvent entraîner un soulèvement et une déformation des pieux qui peuvent endommager le système de rayonnage au-dessus du sol qui supporte les modules photovoltaïques (PV) . Cet article décrit une étude basée sur des données de terrain provenant d'essais de charge axiale et latérale, qui ont été menées pour un projet solaire existant, pour prédire le mouvement global et d'autres paramètres de conception en utilisant à la fois une approche basée sur le code et la méthode analytique semi-empirique, proposée par Ladanyi et Foriero (1998), qui utilise l'équation de Berggren modifiée bien établie (Aldrich et Paynter, 1953) pour calculer la profondeur de congélation. Cela a permis d'évaluer les méthodes de conception actuelles et de mieux comprendre le calcul de routine du taux de pénétration du gel et du soulèvement, ce qui entraîne des forces de soulèvement des pieux. L'étude a révélé des aspects qui nécessitent une étude plus approfondie pour faciliter la conception pratique et économique, et des recommandations pour de futures recherches pour aborder ces aspects sont faites.

1 INTRODUCTION

Solar-generating stations are becoming increasingly economical as a primary energy source. One of the largest risks associated with these facilities is the racking foundation erection due to the potentially large number of members (e.g. a recent project in AB contained up to 250,000 foundation elements). These types of foundation present unique design challenges, with small, closely spaced piles that have low vertical loads. Since the piles are relatively short, near surface climatic effects, such as seasonal ground freezing, snow and wind loading, can lead to frost heaving and deformation of the piles (Levasseur et al, 2015) which can lead to damage to the above-grade racking system which support the photovoltaic (PV) modules. In addition, since the racking system supporting the PV modules are often connected across an entire row, systems may not be very tolerant to differential movement between adjacent supports, which can take place during the freezing and thawing stages of seasonal variations. Ideally, there are no long-term serviceability issues ensuring investors that the asset will generate electricity over its lifetime with minimal operations maintenance.

A range of candidate remedial foundation measures and design approaches have been proposed for use on solar farms, however many of these still need to be fully validated and assessed for long-term use, together with their economic benefits. Design is often optimized to reduce the overall frost uplift effects, but despite this there have been reported cases of poor foundation performance in Ontario on solar farms (Levasseur et al, 2015). This unacceptable foundation behaviour has been attributed to a range of causes, including: frost action, lack of experience, poor geotechnical oversight during construction and difficult piling conditions. With regard to the frost action, the adfreeze forces and frost depths appear to have been improperly estimated. Under-estimation of the frost penetration depth can occur if designers rely on undisturbed snow cover (which reduces frost penetration) and this can be influenced by the wind climate and the presence of the PV modules.

Adfreeze forces can be calculated using the methods outlined in Sections 1.1 and 1.2 below. However, the method outlined in the former of these relies on the estimation of the adfreeze bond stresses (σ).

Recommendations are provided in the CFEM (2006) and the literature (Tomlinson and Woodward, 2008 and Fang, 1991), but these are based on relatively few field tests (e.g. Penner, 1974) and have a rather wide range of values: from 30-270 kPa for steel piles in contact with fine-grained / silty soils. Hence this appears to be a gap in the literature and we need more research in this area.

The current study utilizes field data from axial and lateral load tests, which were conducted for an existing solar project, to predict the overall movement and other design parameters using a code-based approach and a semi-empirical analytical method, proposed by Ladanyi and Foriero (1998), that uses the well-established modified Berggren equation, (Aldrich and Paynter, 1953) to calculate the dept of freezing. This has allowed an assessment of current design methods and more insight into the routine calculation of the rate of frost penetration and heave, resulting in pile uplift forces.

1.1 Design of small piles for frost heave

When soil begins to freeze, it will adhere to any embedded objects (e.g. pile foundations). If this is coupled with ground freezing from frost action, an uplift force will be applied along the embedded structure. This phenomenon is termed 'adfreezing'. Upwards movement of a pile from the adfreeze forces can be counteracted by frictional forces mobilized along the length of the pile below the frost penetration depth (determined during the design).

Frost uplift loads are calculated for different pile configurations and load cases based on the methodology recommended by Becker (2017) and the requirements of the CFEM (2006), using the following equation:

$$F_L = (F_D \times P \times \sigma \times \alpha)/\phi \quad [1]$$

where F_L = frost uplift load. F_D = frost penetration depth, P = pile section perimeter, σ = adfreeze bond stress, α = load factor and ϕ = geotechnical resistance factor.

Frost penetration depth contour maps are available from various bodies (e.g. the Ministry of Transportation of Ontario) and are commonly used for foundation and pavement design in urbanized areas, which assume that the surrounding areas will be maintained and free of snow accumulation and often backfilled with engineered fills, primarily comprising of sand and gravel material that will more readily allow for frost penetration due to the lower thermal resistivity. As such, it is considered necessary to determine the site specific design freezing index, I_d, which can be derived from the mean freezing index, I_m, and equations are provided in the CFEM (2006) to estimate the frost penetration depth (with and without snow cover). This is particularly important, since the design of the foundation elements will often be governed by frost uplift in a cold climate.

1.2 Analytical modelling of frost heave and pile uplift forces

Modelling the process of frost penetration into the ground and the resulting initial heave is highly complex. Various theoretical models have been proposed to predict these phenomena, such as the application of the Clausius-Clapeyron equation by Miller (1972) to develop the "rigid-ice" model and the segregation potential theory proposed by Konrad and Morgenstern (1980). These and other models have been incorporated into computer codes to predict frost heave, e.g. FROST, (Guymon et al. 1993); PC-Heave, Sheng (1994); SSR Model, Saarelainen (1992) and included in finite element programmes for the analysis of complex boundary value problems, such as PLAXIS (Ghoreishian Amiri et al, 2016).

However, to provide accurate predictions these approaches require the determination of a significant number of material parameters that, as has been highlighted above, have to be measured in laboratory tests, obtained from calibration analysis or approximated from data reported in the literature. An alternative approach is to employ semi-empirical methods to provide predictions of rates of frost penetration and frost heave together with the resulting pile uplift forces. This is the approach taken in this study, which is based on the method proposed by Ladanyi and Foriero (1998) for predicting heave stresses acting on piles.

Field studies (e.g. Johnson and Buska, 1988) have indicated that the uplift forces acting on a pile, resulting from adfreeze shear stresses caused by frost heave, are a function of soil temperature along the length of the pile, the displacement rate at the pile-soil interface and the nature of the interface. The method proposed by Ladanyi and Foriero (1998) uses site-specific variations in surface temperature with time in the modified Berggren equation to predict frost penetration and, assuming surface heave is approximately proportional to the depth of frozen soil, predicts the resulting shear stress acting on the pile. The temporal variation in pile uplift force can then be calculated.

2 SITE CONDITIONS AND FIELD TESTS

2.1 Overview

The proposed PV facility is a 32 MW ground mount solar development situated in Alberta. Pre-production load testing and pile design was carried out on the site, which focused on foundation options consisting of helical piles, driven round posts and driven w-section piles. Based on the preliminary investigations, driven W6x9 and/or W8x10 piles were selected to be the foundation supports for the racking system. Hence, a driven pile testing programme was undertaken to assess the suitability of these foundations and to identify areas within the proposed array, where different foundation solutions may be required based on the subsurface conditions and load test results. The site is currently pastureland, with flat to gently undulating topography.

2.2 Site investigation and soil characteristics

Eight geotechnical boreholes were drilled in 2020 using a truck-mounted drill rig and solid stem augers. Based on a review of available surficial geological mapping (McPherson, 1972), glaciolacustrine bedded silt and clay with minor sand overlying glacial till are present on site. The soil profile encountered at the borehole locations generally consisted of firm lacustrine clay with variable plasticity down to borehole termination depths. The clay was often encountered from the surface; however, sometimes a layer

of sand or silt 0.0 m to 3.0 m thick was encountered at the surface. Topsoil was not encountered; however, roots generally extended to depths ranging from 75 to 200 mm below ground surface in all boreholes. A typical borehole record is provided in Table 1 below.

Table 1: Typical borehole data from site

Depth (m)	Description
0-1.8	compact, brown, SAND, fine to medium grained,
1.8-2.3	firm, brown, CLAY , and silt, sandy, low plastic, wet
2.3-3.4	36.3% sand, 42.8% silt & 20.9% clay based
3.4-7.6	medium plastic, trace sand
7.6-9.6	grey, brown colorations
	End of borehole at 9.6 m. Borehole was partially bridging due to soft-firm clay. Water level was at 3.0 m at drilling completion.

Standard penetration tests (SPTs) were also performed at selected depth intervals, and soil samples were obtained from the split-spoon sampler. Groundwater monitoring wells were not installed in all boreholes. The following laboratory tests were completed on soil samples collected from the site: moisture content tests (ASTM D2216), Atterberg limits tests (ASTM D4318), grain size analysis tests (ASTM D422), direct shear tests (ASTM D3080), unconfined compressive strength tests (ASTM D2166), corrosivity tests (i.e., pH, electrical resistivity [ER], oxidation reduction potential [ORP] soluble sulphate and chloride), standard Proctor tests (ASTM D698 – method A) and California Bearing Ratio (CBR) tests (ASTM 1883).

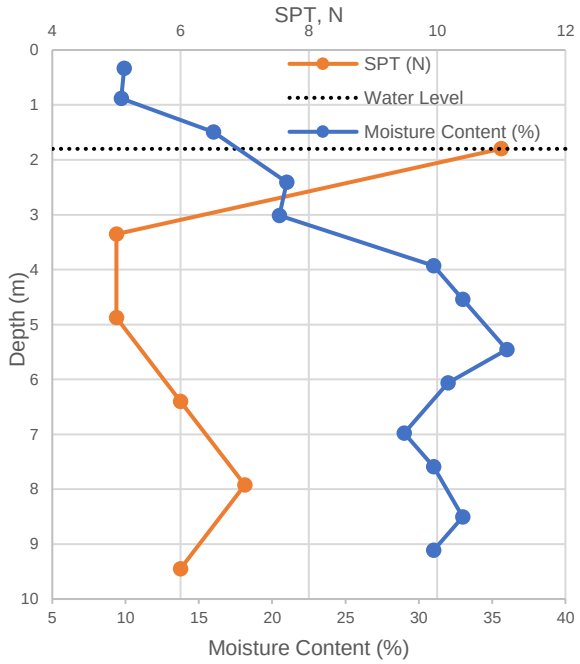

Figure 1. Depth vs moisture content and SPT N for typical borehole with overlying sand stratum.

Sand was encountered in a number of the boreholes. When present, it was encountered at the surface and extended to depths ranging from 0.8 to 2.0 mBGS. The sand was generally fine to medium grained (SM) and silty with variable clay content. The sand was loose to compact in density based on SPT "N" values and brown. Moisture contents of sand samples generally ranged from 6 to 12% indicating dry to moist condition. Typical moisture content and SPT N profiles with depth are shown in Figure 1.

Clay was encountered in all boreholes either from the surface or below the sand stratum and extended until borehole termination depth in all boreholes. The clay generally comprised of greater than 35% silt and variable sand content and was brown turning to grey with depth. Moisture contents on silt samples generally ranged from 15 to 42% indicating moist to wet conditions. SPT "N" values (i.e. blows per 300 mm of penetration) generally ranged from 3 to 9 within the clay which indicates soft to stiff consistency. In general, the clay was within the firm range. Based on the Atterberg and sieve/hydrometer results, the soil is considered to be glaciolacustrine clay; the soil has a large silt component, which is typical for the region of Alberta. Typically, if a soil has at least 20% clay, it will behave cohesively (i.e., it will behave as a clay). Based on the Atterberg limits, the plasticity ranges from low to medium plastic clay which is consistent with the observations made during borehole logging.

Groundwater levels were observed during drilling and at drilling completion at depths ranging from 3.0 m below ground surface (mBGS) to 6.1 mBGS, and as such may not be representative of a stabilized condition. The water table depth is inferred to be related to the loosening of the underlying soils, which is noted based on the reduction in SPT "N" values. Groundwater levels are prone to fluctuations and may be affected by seasonal fluctuations, recent rainfall, surface drainage, and infiltration, etc. The selected geotechnical design parameters from the laboratory and in-situ tests are shown in Table 2, below.

Table 2: Geotechnical design parameters for site.

Parameters	Sand	Clay
Total Unit Weight (kN/m^3)	17.5	16.5
Angle of Internal Friction – Drained (°)	30	20
Undrained Shear Strength s_u (kPa)	N/A	45
Effective Shear Strength, c' (kPa)	N/A	2

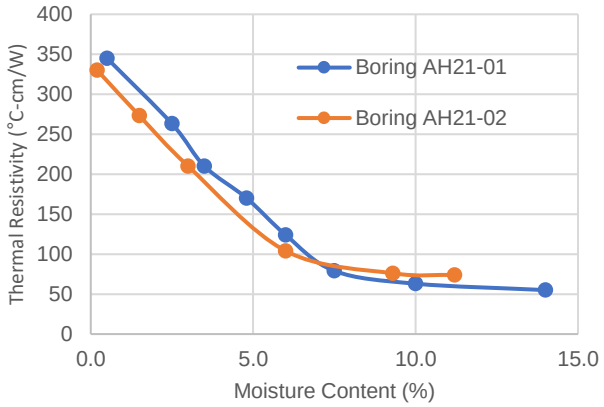

Figure 2. Thermal resistivity vs moisture content

Two thermal resistivity (k) test samples were obtained at approximate depths ranging from 1.2 mBGS to 1.5 mBGS, from the sand stratum. The thermal resistivity testing was performed in general conformance with the Institute of Electrical and Electronics Engineers (IEEE) standard 442. Thermal resistivity testing was completed on the selected bulk samples remolded to approximately 17.3 kN/m^3. These results show typical values for soils of this type and state and the variation of k with moisture content is shown in Figure 2.

2.3 Axial pile pullout testing and design

Piles were driven on site using a Mazaka MW 1200 driven pile rig with a 1450 joule hammer, with an installation capacity of 350 to 700 blows per minute, advanced under full-time supervision of the engineers. Forty driven W8x10 piles were installed adjacent to the main array piles for the purposes of load testing immediately after installation and to compare results to piles with rest time of a minimum of 72 hours prior to testing. Pile locations were predrilled/augered through the frost penetration depth of approximately 2.1 m. The testing was completed to mechanically mimic applied snow loads, loads, frost uplift and eccentric wind loadings with an appropriate factor of safety and were completed to evaluate the pile ultimate capacities, and ultimately develop an optimised foundation design. Lateral tests were completed following the axial testing.

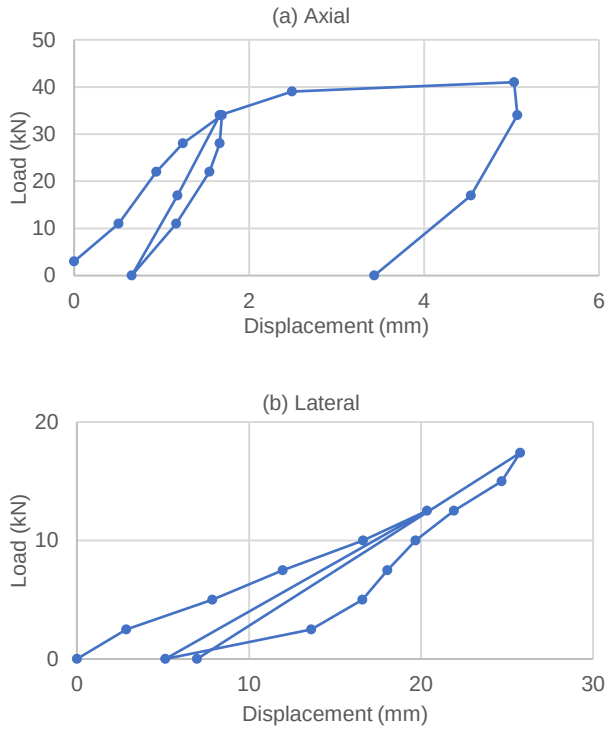

Figure 3. Axial and lateral load tests for pile LT21-23

Axial load testing was conducted using a hydraulic jack mounted to a reaction frame. The failure criteria for the axial test piles were a maximum vertical displacement of 25 mm, residual vertical displacement of 12.5 mm upon completion of unloading and pile creep of 0.1 mm/min or lower under the frost design load. For lateral loading, maximum lateral displacement of 25 mm and residual lateral displacement of 12.5 mm. Typical pile loading tests are shown in Figures 3(a) and (b), which show a relatively elastic response to the axial design load of 35 kN with the foundation then moving into a plastic response zone beyond this load increment. During lateral load testing while the maximum deflection was exceeded, since residual deflection was below the allowable limit it is inferred that lateral loading will not permanently deform the foundation. Furthermore. these excessive lateral deflections are considered acceptable as long as the differential lateral movement does not exceed the lateral differential tolerance of the racking system which will transfer stresses to the racking system causing permanent deformation.

The average design parameters determined from the pile load test programme are shown in Table 3. Site specific mean and maximum frost depths were calculated for the designs and the inferred frost uplift forces adjusted based on the engineering calculations. Table 4 below summarizes the finalized parameters and resulting frost uplift loads for each test pile configuration used in the pre-production test investigation. The frost loads for the W-section piles were calculated using a resistance factor (ϕ) of 0.6 and a load factor 1.25 with a frost depth of 1.7 m.

Table 3: Unfactored design parameters for driven W piles

Approximate Depth (mBGS)	Unfactored Ultimate Shaft Resistance (kPa)	Unfactored Ultimate Toe Resistance (kPa)
0 to 2.1	10	16.5
2.1 to 6.3	19	20
6.3 to 9.6	N/A	45

Table 4: Frost load summary for W-section piles

Pile Cross-Section	Cross-Section Perimeter (m)	Adfreeze/ Friction Bond (kPa)	Coeffi-cient of Friction	Frost Uplift Load (kN)
W6x9	0.691	65	1.0	159
W8x10	0.792	65	1.0	182

Based on the above pile resistance data and frost uplift calculations, lateral design of the racking foundations is suggested to be governed by racking-induced lateral loading, whereas axial design would be governed by frost uplift. Comparing the values of shaft friction in Table 3 with the adfreeze friction bond in Table 4, it is clear that in order to resist uplift, piles have to be installed to significant depths below the seasonally frozen active layer or other solutions employed to either reduce adfreeze friction (such as friction reduction sleeves) or increase pile capacity (such as installing helical piles). However, in order to arrive at economic design solutions it is necessary first to be able to predict frost uplift loads reliably.

3 PREDICTION OF FROST HEAVE IN FIELD TESTS

3.1 Method of analysis

As outlined above, the method originally developed by Ladanyi and Foriero (1998) was used to predict pile frost heave. In this method the temporal variation in frost penetration is predicted using the semi-empirical modified Berggren equation. This was developed by Aldrich & Paynter (1953) and is used widely in practice, e.g. Canadian Foundation Engineering Manual (Canadian Geotechnical Society, 2006). The depth of frost penetration at a given time, $x_o(t)$, is a function of the freezing index, $I_f(t)$, as given by:

$$x_o(t) = \omega\sqrt{I_f(t)} \quad [2]$$

in which

$$\omega = 60\lambda\left(\frac{48k_{av}}{L}\right)^{1/2} \quad [3]$$

where λ is the correction coefficient in the modified Berggren equation (e.g. Andersland and Ladanyi, 2004); k_{av} is the average soil thermal conductivity (W/mK); and L is the latent heat of fusion (MJ/m^3).

Measurements obtained from a weather station located close to the proposed solar power plant were used for the surface temperature boundary condition in the analysis. The annual temperature variation data recorded at this station can be approximated closely using a sine curve, as shown in Figure 4. This data is used to calculate the freezing index, $I_f(t)$, and, from equations 2 and 3 the depth of frost penetration with time, $x_o(t)$ is predicted.

To predict the rate of heave Ladanyi and Foriero (1998) adopted the finding of Saarelainen (1992) who observed in field studies that surface heave, s_s, is approximately proportion to the thickness of the freezing layer, i.e.

$$s_s(t) = Kx_o(t) \quad [4]$$

where K is the coefficient of proportionality.

In the analysis presented herein, the value of K was obtained from measurements of surface heave and depth of frost penetration reported by Penner (1974). Similar values have been reported for a range of soil types, e.g. Saarelainen (1992). Equation 4 allows the evolution of surface heave to be predicted.

The relative displacement rate at the pile soil interface, $\dot{s}_i$, is obtained from the differentials of equations 2 and 3. This allows calculation of the mobilised tangential stress, $\tau_{a,i}$, at a depth x_i , from:

$$\tau_{a,i} = \tau_{c,\theta i}\left[\frac{n-1}{\dot{\gamma}_c}\right]^{1/n}\left[\frac{\dot{s}_i(t)}{a}\right]^{1/n} \quad [5]$$

where a is the pile radius, n is the creep exponent, $\dot{\gamma}_c$ an arbitrary reference shear strain rate and $\tau_{c,\theta i}$ the shear creep modulus that is related to the general creep modulus, σ_{c0} , and temperature through:

$$\tau_{c,\theta} = \sigma_{c0}\left(1 + \frac{\theta}{\theta_0}\right)^w \quad [6]$$

in which θ is the absolute value of the negative temperature, $\theta_0 = 1$°C, and w the experimental temperature exponent. The parameters, *n*, *w* and σ_{c0} are obtained from laboratory element tests. For the analyses reported herein typical values of these parameters for ice rich silt obtained from the literature have been used (Andersland and Ladanyi, 2004) and these are given in Table 5 together with the other paraments used in the analysis. The pile is a W-section (W8x10) that has a cross section perimeter of 0.792m.

Values of mobilised tangential stress, $\tau_{a,i}$, acting on the pile are obtained using a number of time steps and are integrated over the surface area of the pile to obtain the uplift heave force. At each time step, the frost penetration and frost penetration rate together with the surface heave and heave rate, are obtained from which the relative displacement rate at the pile soil interface, $\dot{s}_i(t)$ can be computed and, hence, the mobilised tangential stress, $\tau_{a,i}$, determined using equation 5. Weaver and Morgenstern (1981) proposed that the mobilised tangential stress is affected by both the material forming the pile (i.e. concrete or steel) and its surface properties (i.e. smooth or ridged). For smooth steel piles, as in the analysis conducted herein, Weaver and Morgenstern (1981) suggested a reduction factor of 0.6, and this has been used in the analysis.

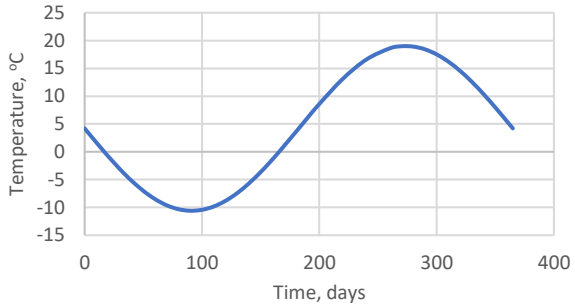

Figure 4. Daily temperature variation used in analysis (based on data provided by Government of Canada)

Table 5. Parameter values used in the analyses

Parameter	Value
Average moisture content, %	10.0
Latent heat of fusion, L (MJ/m^3)	54.166
Average soil thermal conductivity, k_{av} (W/m.K)	1.350
Correction coefficient, λ	0.85
Creep exponent, *n*	3
Experimental temperature exponent, *w*	0.37
General creep modulus, σ_{c0}	0.103

3.2 Results of analysis

Predictions of the time variation in the average uplift shear stress acting on pile and of uplift heave force on the pile during a period of freezing are presented in Figures 5 and 6, respectively. Each figure displays two sets of data, i.e. (i) for conditions in which no slip is experienced at the

interface between the frozen soil and the pile, and (ii) where slip occurs when the relative displacement between the frozen soil and the pile is calculated to be greater than 2 cm. For the latter case, Johnston and Ladanyi (1972) observed in rod anchor pullout tests that at this relative displacement the adfreeze strength reduced by 50%. Where appropriate, this factor has been applied to the no slip values of mobilised tangential stress.

The results indicate that as the depth of the freezing front increases and uplift shear stresses act over an increasing depth of the pile the resulting heave force initially increases, as shown in Figure 6. The mobilised shear stress is a function of the relative displacement rate at the pile soil interface, $\dot{s}_i(t)$, and this reduces with time to zero when the surface air temperature increases to 0°C (at 166 days). As the depth of the freezing front increases the length of pile subjected to uplift shear stresses increases. The net result is that the peak uplift heave force occurs a short time *after* the surface temperature reaches its minimum value (at 90 days, see Figure 4).

From Figure 5, it can be seen that the maximum average shear stress acting on the pile is 186 kPa when there is no slip. In contrast, the shear stress on the pile reduces to 103 kPa when there is slip. The maximum uplift forces acting on the pile are 191 kN and 101 kN for the no slip and slip conditions, respectively, as seen in Figure 6. Comparison of values in Figures 5 and 6 indicates that when the uplift forces are at their maximum (at 110 days) the average shear stresses acting on the pile are 163 kPa and 85 kPa for the no slip and slip conditions, respectively.

3.3 Discussion

To date very few experimental site studies have been conducted to investigate adfreezing on piles. The most comprehensive of these reported in the literature was conducted by Penner (1974), who calculated values of uplift shear stress acting on piles ("adfreeze bond stress") from measurements of uplift force. In this study it was observed that, for fine-grained soils frozen to steel piles, the average value of uplift shear stress acting on the pile ("adfreeze bond stress") ranged between 62 kPa and 172 kPa; at the peak recorded value of frost uplift heave force the average shear stress acting on the pile was 72 kPa. Based on Penner (1974), the Canadian Foundation Engineering Manual suggests using an adfreeze bond value of 100 kPa for fine-grained soils frozen to steel piles to predict frost uplift load. For similar conditions, Penner and Gold (1971) reported an adfreeze bond value of 113 kPa. More recently, (Levasseur et al., 2015) estimated the adfreeze bond stress acting on H-piles that were supporting solar panels at a site in southwestern Ontario. This was achieved by calculating the adfreeze forces required to overcome the shaft resistance of a pile. From this, they estimated the adfreeze bond stress ranged between approximately 30 kPa and 80 kPa.

Code-based values of frost uplift load calculated using Equation 1 above (as recommended in CFEM, 2006), are presented in Table 4. Comparing the uplift load for the W8x10 piles with the predictions using the semi-empirical analytical method described herein (Ladanyi and Foriero, 1998), the CFEM method predicted an uplift load of 182 kN, whilst the analytical method indicates maximum uplift forces of 191 kN and 101 kN for the no slip and slip conditions, respectively (Figure 6). However, it should be noted that the value calculated using the CFEM method is *factored* (for use in design). If the load factor, α, and geotechnical resistance factor, ϕ are both set to unity, the *unfactored* value of uplift load is found to be 88 kN.

Hence the values of maximum average shear stress acting on the pile predicted by the codified and more rigorous, semi-empirical model are, therefore, within the range of available published data. However, the more complex analytical approach suggests that these predictions will vary with soil moisture content, water table location, ice creep rate, rate of freezing and other geometric and material properties of the piles. Thus further work is required to validate reliable methods of prediction that are not overly conservative. In addition, the analyses described have assumed the interaction of the *full* perimeter of the W-section piles. However, it is common practice in geotechnical engineering to include the presence of a soil plug, when calculating shaft friction resistance and account for this by using the outside (box) perimeter of the pile instead. The formation of a plug can occur between the flanges and the web of a W-section pile during installation, changing the driving behaviour and the subsequent axial frictional response. There are differing opinions as to the conditions when this will occur. Tomlinson and Woodward (2008) suggest a W-pile driven in silty and sandy soils will *not* form a soil plug, but the Federal Highway Administration (FWHA 2006), assume that a plug will be formed in fine and coarse-grained soils. This aspect also requires further investigation.

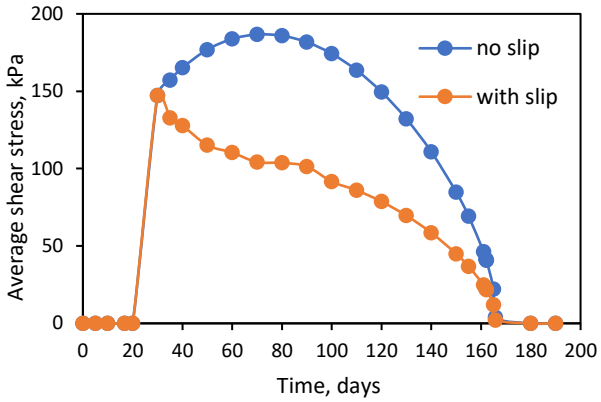

Figure 5. Predicted time variation of average uplift shear stress acting on pile

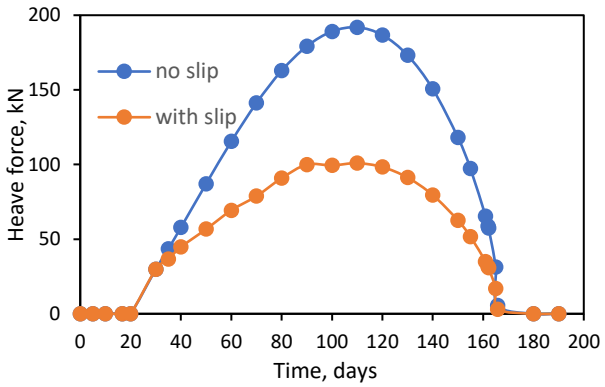

Figure 6. Predicted time variation of uplift heave force on the pile

4 CONCLUSIONS

The findings of this study indicate that whilst lateral design of the racking foundations is governed by lateral loading induced by the racking, axial design of the piles supporting the racking is governed by frost uplift. In order to minimise displacements resulting from piles heaving as a result of frost uplift, it is necessary to reliably predict frost heave induced uplift loading on piles together with validating and assessing practical, economic solutions to resist this loading. The simple prediction of frost uplift loading has been addressed in this paper.

In an analysis based on the method proposed by Ladanyi and Foriero (1998), there was reasonably close agreement between the values of average uplift shear stress acting on the pile at the point of maximum uplift force predicted by the model, the CFEM and that reported by Penner (1974), of 85 kPa and 72 kPa, respectively. Whilst this is a most encouraging result, these comparisons are based on extremely limited field data and some of the key parameters in the model were obtained from the literature. It may be concluded, therefore, that rigorous validation of the proposed method of analysis is required that should involve further field and laboratory studies.

ACKNOWLEDGEMENTS

The authors wish to thank NSERC for the funding of Mr. Hammad for their support during this study.

REFERENCES

Aldrich, H.P. and Paynter, H. M. 1953. *Analytical Studies of Freezing and Thawing of Soils*, Technical Report No. 42, Arctic Construction and Frost Effects Laboratory, New England Division U.S. Army Corps of Engineers, Boston, MA, U.S. Arctic Construction and Frost Effects Lab Boston Ma., USA.

Andersland, O.B. and Ladanyi, B. 2004. *Frozen Ground Engineering*, 2nd Edition, John Wiley & Sons.

Becker, D. 2017. Geotechnical Risk Management and Reliability Based Design - Lessons Learned. *Geo-Risk 2017* Conference, June 4-7, Denver, Colorado.

Canadian Geotechnical Society, 2006. *Canadian Foundation Engineering Manual,* 4th Edition.

Fang, H-Y, 1991. *Foundation Engineering Handbook*. 2nd Edition, Van Nostrand Reinhold, New York, NY, USA.

Ghoreishian Amiri, S.A., Grimstad, G., Kadivar, M., Nordal, S. 2016. Constitutive model for rate-independent behavior of saturated frozen soils, *Canadian Geotechnical Journal*, 53: 1646–1657.

Guymon, G.L., Berg, R.L., and Hromadka, T.V. 1993. Mathematical Model of Frost Heave and Thaw Settlement in Pavements. *CRREL Report 93-2*, U.S. Army Corps of Engineers Cold Regions Research and Engineering Laboratory, Hanover, NH, USA.

Johnson, J.B. and Buska, J.S. (1988). *Measurement of frost heave forces on H-piles and pipe piles*, CRREL Report 88-21, 49 p.

Johnston, G. H. and Ladanyi, B. (1972), Field tests of grouted rod anchors in permafrost, *Canadian Geotechnical Journal*, 9, 2, pp. 176-194

Konrad, J.-M. and Morgenstern, N.R. 1980. A mechanistic theory of ice lensing in soils. *Canadian Geotechnical Journal*, 17(4): 473-86.

Ladanyi, B., and A. Foriero. 1998. Evolution of frost heaving stresses acting on a pile. *Proceedings of the 7th International Conference on Permafrost*, Yellowknife, Canada, 623-634.

Levasseur, P.-P., Maher, M. and Dittrich, J.P. 2015. A case study of frost action on lightly loaded piles at Ontario solar farms, *GeoQuebec 2015*, Proceedings of 68th Canadian Geotechnical Conference and 7th Canadian Permafrost Conference, Québec, Canada.

McPherson, R.A. 1972. Surficial geology of the northern Foothills. Research Council of Alberta.

Miller, R.D. 1972. Freezing and heaving of saturated and unsaturated soils. *Highway Research Record*, 393: 1-11.

Penner, E. (1974). Uplift forces on foundations in frost heaving soils. *Canadian Geotechnical Journal*, 11(3), 323-338.

Penner, E. and Gold, L. W. (1971) Transfer of heavy forces by adfreezing to columns and foundation walls in frost-susceptible soils, *Canadian Geotechnical Journal*, 8, pp. 514–26.

Saarelainen S. 1992. *Modelling frost heaving and thaw penetration at some observation sites in Finland. The SSR model*. PhD Thesis, Tampere University of Technology, Finland, VTT Publications 95. 1

Sheng, D. 1994. *Thermodynamics of Freezing Soils: Theory and Application*. Doctoral thesis, Luleå University of Technology, Sweden.

Tomlinson, M., & Woodward, J. 2008. *Pile design and construction practice* (5th ed.). Taylor & Francis, New York, NY, USA.

Weaver, J.S. and Morgenstern, N.R. (1981). Pile design in permafrost. *Canadian Geotechnical Journal*, 18(3), 357-370.